Research Article GU J Sci 34(4): 1179-1191 (2021) DOI: 10.35378/gujs.798695

Gazi University

Journal of Science

http://dergipark.gov.tr/gujs

Optical Properties of Gaas/Al_xga_{1-X}as Superlattice Under E-Field for Quantum Cascade Laser Application

Behcet Ozgur ALAYDIN[1,2,*]

[1] *Nanophotonic Research and Application Center, Cumhuriyet University, 58140 Sivas, Turkey*
[2] *Faculty of Science, Department of Physics, Cumhuriyet University, 58140 Sivas, Turkey*

Highlights

- This paper focuses on optical properties of superlattice for quantum cascade laser applications.
- Effect of electric field intensity and quantum well thickness are studied to obtain wave functions.
- Finite difference method (FDM) is utilized to solve 1d-Schrodinger equation.

Article Info

Received:22 Sep 2020
Accepted:09 Jan 2021

Keywords

Superlattice
Quantum cascade laser
Optical properties
Electric field
GaAs/$Al_xGa_{1-x}As$

Abstract

Optical properties of GaAs/$Al_xGa_{1-x}As$ superlattice are studied dependent on quantum well thickness of gain region and doping density of injector layers underperformed electric field. Conduction band alignment of the superlattice is obtained by using effective mass approximation. 1d-Schrodinger formula is solved by using FDM. Intersubband transition energies, linear (nonlinear and total) absorption coefficients and linear (nonlinear and total) refractive index changes are plotted under applied electric field intensity. Intersubband transition energy of electron from second excited state to first excited state shows 147 meV. It is found that -45 kV/cm electric field intensity and 5 nm layer thickness of last quantum well of the gain region are the best values for studied structure. After that, linear absorption coefficient is investigated dependent on carrier number in the injector region under electric field. It is found that carrier number over $5\ x\ 10^{16}\ cm^{-2}$ can causes huge internal absorption of the radiative emission obtained in gain region due to increase in linear absorption coefficient by factor 10. As a conclusion, total absorption coefficient and total refractive index change are calculated for optimized parameters.

1. INTRODUCTION

Since couple of last decades, there has been very much interest to low dimensional quantum mechanical systems. Especially, quantum well (QW), wire and dot (QD) multi heterostructures are under extensive research owing to their tremendous optical, structural and electrical properties. The studies about these structures lead to a novel area in solid state physics. This results in many possible applications for electronic and opto-electronic devices such as high-speed electron-optical modulators [1], current controlled transistors [2], near and mid-infrared detectors [3] and semiconductor lasers [4]. Owing to the broad diversity of industrial applications, multi QWs have been broadly studied for different conditions such as hydrostatic pressure, temperature, electric, magnetic and laser fields, different doping processes and etc. [5–9]. Under these conditions, it is possible to modify subband energies and their corresponded wave functions. Thus, energy levels are occurred in the QWs with confined carriers and this causes mainly seeing nonlinearities in the semiconductor structure compared with bulk materials [10,11].

In the last years, superlattices (SL) have attracted considerable attention because of their important electronic and optical properties and possible practical applications [12-15]. Sirtori et. al. [16] have grown SL by molecular beam epitaxy (MBE) and have studied its lasing performances for quantum cascade laser (QCL). Razeghi et. al. [17] have studied a superlattice (SL) for different band arrangements. Then they have compared theory with experimental data. The absorption coefficient (linear-LIN, nonlinear-NLIN and total) of superlattice under electric field (e-field) is calculated by Shi et. al. [18].

* e-mail: balaydin@cumhuriyet.edu.tr

The optical properties of one-dimensional semiconductor composite structures have been deeply analyzed in the last two decades [19–25]. Radu [19] has examined the laser dressing of energy states in grading semiconductor layer arrangement. Optical rectification of strained $In_xGa_{1-x}N/Al_yGa_{1-y}N$ quantum well by considering influence of the spontaneous and piezoelectric polarization fields on the potential profile is studied by Karimi and Vafaei [20] and also, they work on the frequency conversion. Zeiri et al. [21] study intrasubband NLIN optical properties in asymmetric (Cadmium Sulfide/Zinc Selenide - CdS/ZnSe) QWs. Keshavarz et. al. [22] work on LIN and NLIN intrasubband optical absorption for double semiparabolic QW. Refractive index changes and absorption coefficients are calculated asymmetric double QW in a GaAs by Rodriguez et al. [23]. Ungan et al. [26,27] have deeply investigated effect of different confinement potentials on optical properties of QW. As a result, all referred works in this paper have not been considered only for their physical shapes, there are important effects of physical shapes on the optical properties of semiconductor layer arrangements. Nevertheless, even published many papers to analyze MQWs (multi-quantum well), Superlattices are not studied extensively except for limited number of studies [28] to examine optical properties.

In this work, optical properties of the $GaAs/Al_{0.33}Ga_{0.67}As$ SL for QCL is studied depending on superlattice thickness and carrier number under applied electric field. Intersubband transition energies, dipole matrix elements, LIN, NLIN and total absorption coefficients and LIN (NLIN and total) refractive index changes are found for E_{21} and E_{32} transitions. In the calculations, almost the same experimentally grown hetero structure by Sirtori et. al. is studied. Effective mass approximation is considered in numerical calculations and 1d-Schrodinger equation is solved by utilizing FDM.

2. THEORY

In this research, $GaAs/Al_{0.33}Ga_{0.67}As$ based superlattice is designed and study is done perpendicular to growth plane. Superlattice is split into two part as active region (gain) and electron source (injector) regions. Quantum mechanical calculations are done independently due non-interaction of the quantum energy levels. Gain region has asymmetric triple quantum wells and injector region has asymmetric five quantum wells. E-field is chosen as $\vec{F} = F\vec{z}$. In this condition, Hamiltonian is described as [29];

$$H = \frac{\vec{p}^2}{2m^*} + V(z) + eF\vec{z}\,. \tag{1}$$

Symbol m^* represents effective mass of electron, which is used as $0.067m_0$. Free electron mass is represented as m_0. Square of momentum operator and electron charge are symbolized as $\vec{p}^2$ and e. $V(z)$ is the SL quantum barrier height in energy. For $GaAs/Al_{0.33}Ga_{0.67}As$ system conduction band offset is taken as 0.6 and potential discontinuity $V(z)$ is 0.228 meV. To solve Equation (1), eigenfunctions of the infinite QW is used as given below for well width L;

$$\psi_n(z) = \sqrt{\frac{2}{L}}\cos\left(\frac{n\pi z}{L} - \delta_n\right) \tag{2}$$

where δ_n is;

$$\delta n = \begin{cases} 0, n\ is\ odd \\ \frac{\pi}{2}, n\ is\ even \end{cases}. \tag{3}$$

After deriving the energy states and corresponded wave functions, LIN and NLIN absorption coefficients are calculated as follow [30]:

$$\beta(w) = w\sqrt{\frac{\mu}{\varepsilon_r}}\frac{|M_{ij}|^2\sigma_v\hbar\Gamma_{ij}}{(\Delta E_{ij}-\hbar w)^2+(\hbar\Gamma_{ij})^2} \tag{4}$$

$$\beta^{(3)}(w,I) = -2w\sqrt{\frac{\mu}{\varepsilon_r}}\left(\frac{I}{\varepsilon_0 n_r c}\right)\frac{|M_{ij}|^4\sigma_v\hbar\Gamma_{ij}}{((\Delta E_{ij}-\hbar w)^2+(\hbar\Gamma_{ij})^2)^2}\left(1-\frac{|M_{jj}-M_{ii}|}{|2M_{ii}|^2}\frac{(\Delta E_{ij}-\hbar w)^2-(\hbar\Gamma_{ij})^2+2\Delta E_{ij}(\Delta E_{ij}-\hbar w)}{\Delta E_{ij}{}^2+(\hbar\Gamma_{ij})^2}\right) \tag{5}$$

where w represents the angular frequency and Γ_{ij} is relaxation time for intersubband transitions. μ and ε_r symbolize the magnetic permeability and real side of the electrical permittivity. σ_v is the electron density, ħ is Planck constant and transition energy is defined as ΔE_{ij} between excited and ground energy state of the electron. M_{ij} corresponds to transition dipole element and it is given as [31];

$$M_{ij} = \int \psi_j(z)^* \, |e| \, z \, \psi_i(z) \, dz \ . \tag{6}$$

Sum of LIN and NLIN is defined as total absorption coefficient and it is written as given below;

$$\beta(w,I) = \beta^{(1)}(w) + \beta^{(3)}(w,I) \ . \tag{7}$$

The LIN and NLIN refractive index change are formulated as [32]:

$$\frac{\Delta n(w)}{n_r} = \frac{|M_{ij}|^2 \sigma_v}{2 n_r^2 \varepsilon_0} \left[\frac{\Delta E_{ij} - \hbar w}{(\Delta E_{ij} - \hbar w)^2 + (\hbar \Gamma_{ij})^2} \right] \tag{8}$$

$$\frac{\Delta n^{(3)}(w,I)}{n_r} = -\frac{\mu c |M_{ij}|^2}{4 n_r^3 \varepsilon_0} \frac{\sigma_v I}{\left((\Delta E_{ij} - \hbar w)^2 + (\hbar \Gamma_{ij})^2\right)^2} \left[4\left(\Delta E_{ij} - \hbar w\right)|M_{ij}|^2 - \frac{\left(M_{jj} - M_{ii}\right)^2}{\Delta E_{ij}{}^2 + \left(\hbar \Gamma_{ij}\right)^2} \{ \left(\Delta E_{ij} - \hbar w\right) \Delta E_{ij} \left(\Delta E_{ij} - \hbar w\right) - \left(\hbar \Gamma_{ij}\right)^2 (2\Delta E_{ij} - \hbar w) \} \right] . \tag{9}$$

Finally, sum of LIN and NLIN gives total refractive index change, which is expressed as;

$$\frac{\Delta n(w,I)}{n_r} = \frac{\Delta n^{(1)}(w)}{n_r} + \frac{\Delta n^{(3)}(w,I)}{n_r} \ . \tag{10}$$

3. RESULTS AND DISCUSSIONS

The variables utilized in the work are as follow; $m^* = 0.067 m_0$, $V_0 = 228\ meV$, $I = 0.4\ MW/cm^2$ $\mu = 4\pi\ x\ 10^{-7}\ H\ m^{-1}$, $\sigma_v = 1\ x\ 10^{16}\ cm^{-2}$, $\tau_{21} = 0.14\ ps$, $\tau_{32} = 2.4\ ps$ $\Gamma_{ij} = 1/\tau_{ij}$ and $n_r = 3.3254$. We have divided SL into two part. First, we focus on asymmetric gain region then we consider injector region. For the gain region, thickness (L) of the last quantum well is changed under applied electric field intensity. Schematic of the conduction band diagram of the SL for different F values are plotted in Figure 1.

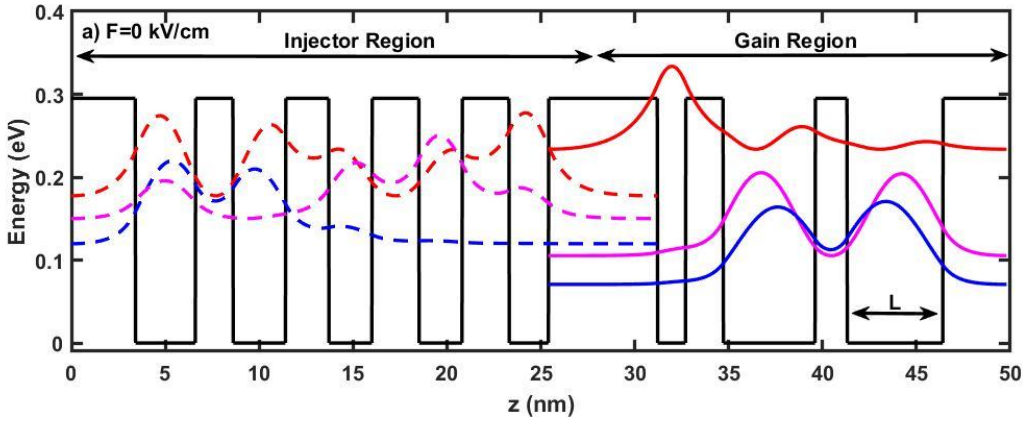

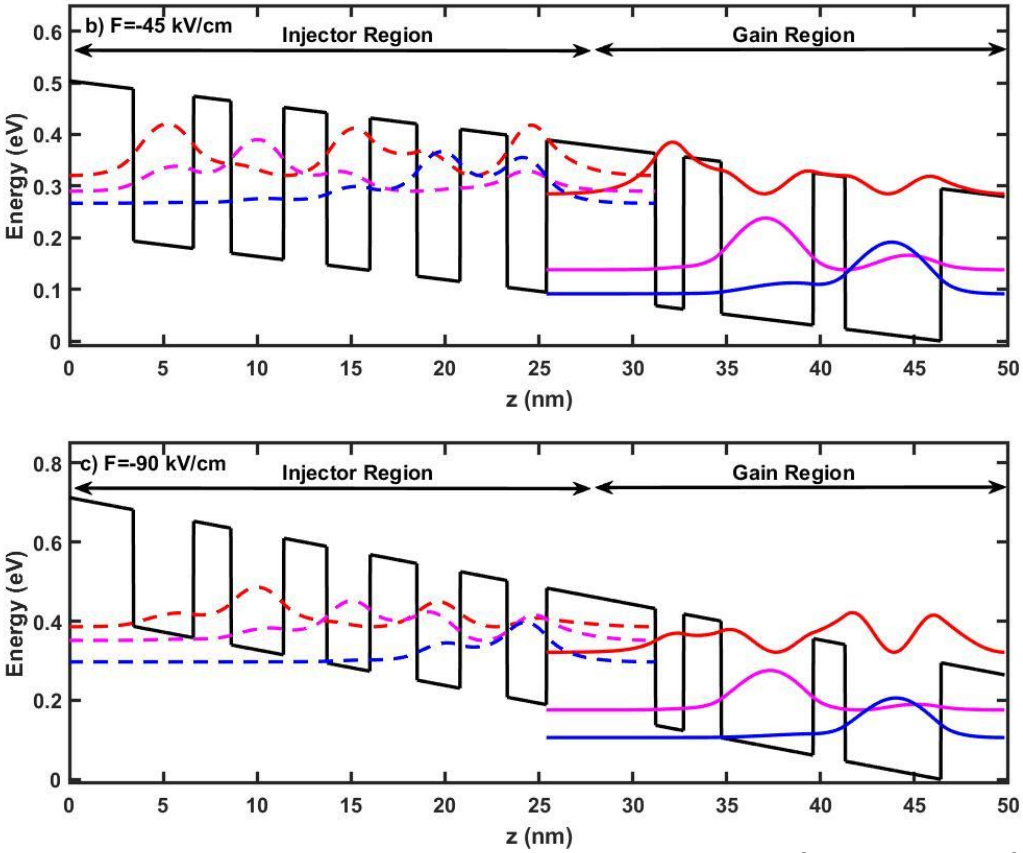

Figure 1. *Conduction band diagram and energy levels of SL for (a)* $F = 0\ \frac{kV}{cm}$*, (b)* $F = -45\ \frac{kV}{cm}$ *and (c)* $F = -90\ \frac{kV}{cm}$

Thicknesses are in nm scale and layers are as follow (from left to right) for one period SL: 3.4/**3.2**/2.0/**2.8**/2.3/**2.3**/2.5/**2.3**/2.5/**2.1**/5.8/**1.5**/2.0/**4.9**/1.7/$\boldsymbol{L(4.5-5.5)}$ nm. QWs are in bold, barriers are in normal font. The underlined layers are doped layers of injector section. When applied electric field intensity is zero, ground and first excited energy states are localized in the middle and right quantum well in the gain region due to thicker wells (Figure 1(a)). Second excited energy state is localized in the first thin quantum well. Electric field affects the localizations in the quantum wells (Figure 1(b)). Ground state localizes in the last well in gain while first excited energy state is localized in the middle quantum well. As an effect of electric field, localization of the second excited energy state decreases in the first thin well in gain and distributed to all wells. When electric field intensity is increased further, separation in localization of the ground and first excited energy states becomes more pronounced in gain and second excited energy state starts to localize in the last well more (Figure 1(c)). While ground, first and second excited state energies are increasing proportionally with electric field, transition energies $E_{21} = 70\ meV$ and $E_{32} = 146\ meV$ are almost constant. This unchanged feature is very important for QCL applications because emission wavelength is kept constant. On the other hand, E_{32}transition probability is increasing with electric field intensity at first but excess increase of the electric field causes localization of electrons in the third quantum well more, that decreases probability of E_{32} transition because second excited energy state start behaving like unbounded energy state that causes electron leakage so this destroys probability of radiative recombination in the gain region. So that this limits maximum working voltage of QCL. E_{21} transition energy is $36\ meV$ which is higher than longitudinal mode energy in GaAs. This enables non-radiative electron transition from first excited state to ground energy state with energy relaxation by phonon vibrations. So that, continuous electron flow from gain region to injector region is possible. Same as in gain, applying electric field also increases ground, first and second excited energy states in the injector region. When ground state is localized at the left side of the injector region, second and third energy levels distributed through injector region. As electric field is applied, localization of the ground state is shifting toward gain. With the help of electric field, ground state of injector and second excited state of the gain are

leveling so that electron tunneling between these states becomes possible. This is main purpose of using injector region in QCL structures so that one electron involves more than one radiative transition after each tunneling to active region.

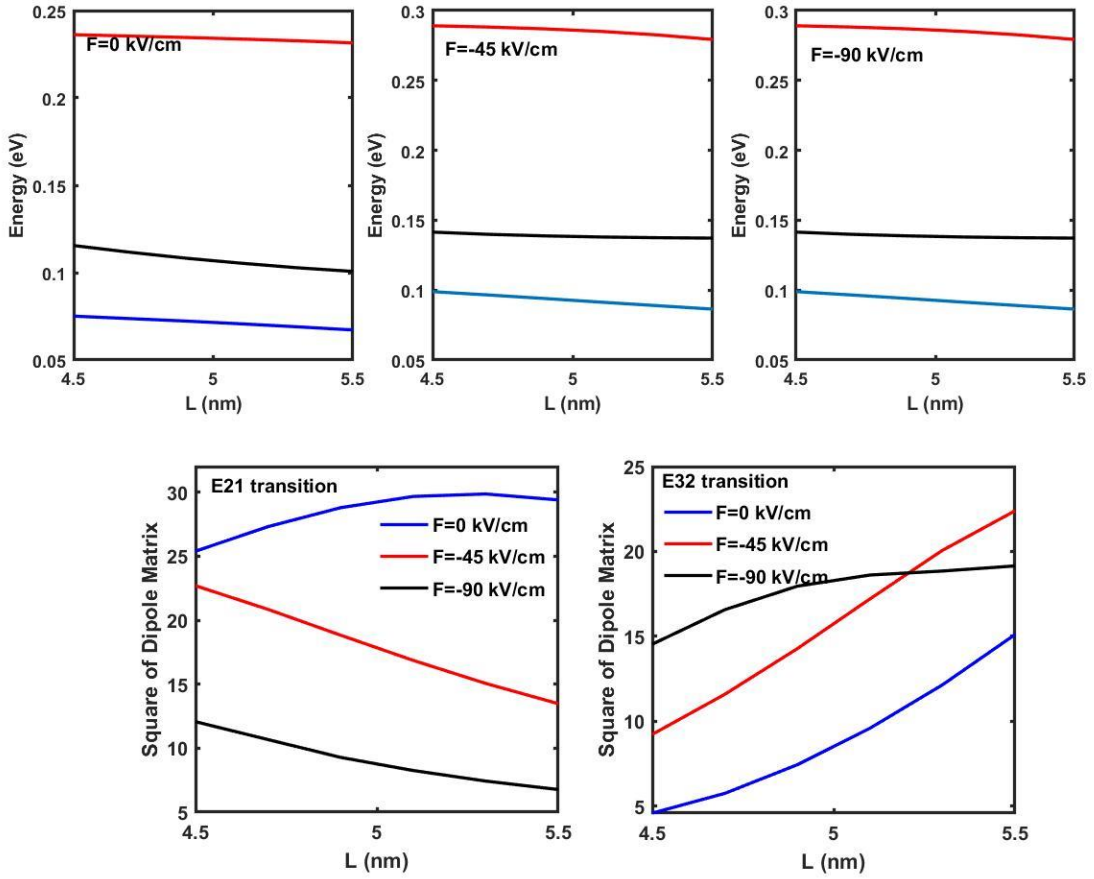

Figure 2. *L versus (a) state's energy variation for different electric field values (upper) and (b) square of dipole matrix element (lower)*

As expected, energy is inversely proportional with L but almost the same change happens for all energies so that L has negligible effect on radiative transition value (Figure 2). On the other hand, radiative transition probability is proportional with L for zero field and $-45\ \frac{kV}{cm}$ electric field value owing to enhanced overlapping of wave functions. However, $-90\ \frac{kV}{cm}$ electric field and thicker L have limited effect on square of dipole matrix element because of that increasing quantum well does not contribute radiative transition anymore. While increasing L results in lower square of dipole matrix element for E_{21} transition, change dependent on the electric field has the same ratio for $-45\ \frac{kV}{cm}$ and $-90\ \frac{kV}{cm}$. Also, higher electric field has lower square of dipole matrix element which is not desired for continuous electron flow in the conduction band. In the end, change in square of dipole matrix element for E_{21} and E_{32} are factor -2 and 2. In this case, optimum value for quantum well thickness is around 5 nm for the last quantum well in the gain region.
In this part of the paper, optical properties of the injector and gain region is discussed. Linear absorption coefficient and refractive index change are investigated by means of L and carrier number under applied electric field.

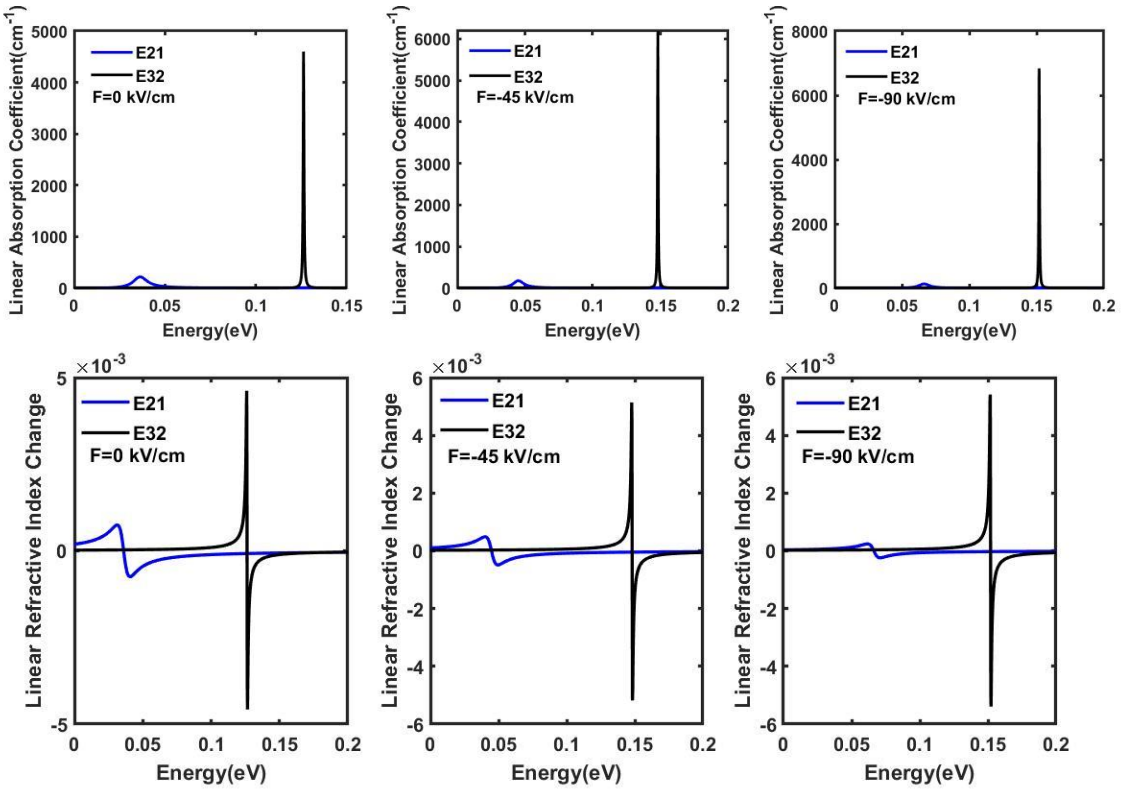

Figure 3. *Energy versus (a) linear absorption coefficient (upper) and (b) refractive index (lower) change for different electric field values in gain region.* $L = 5\ nm$ *and* $\sigma_v = 1\ x\ 10^{16}\ cm^{-2}$*are taken*

As shown in Figure 3(a), linear absorption coefficient is increasing with electric field for radiative E_{32} transition. At the same time, it is decreasing for E_{21}transition. High value of the absorption coefficient can have big impact on output power of QCL because of internal absorption. So that as much as low absorption coefficient is desired. Linear absorption coefficient is decreasing with increased electric field intensity for E_{21}, that is a good indication for higher emission. Moreover, electric field has no major effect on the linear refractive index Figures 3(b). Change in linear refractive index is negligible small for all electric field intensity.

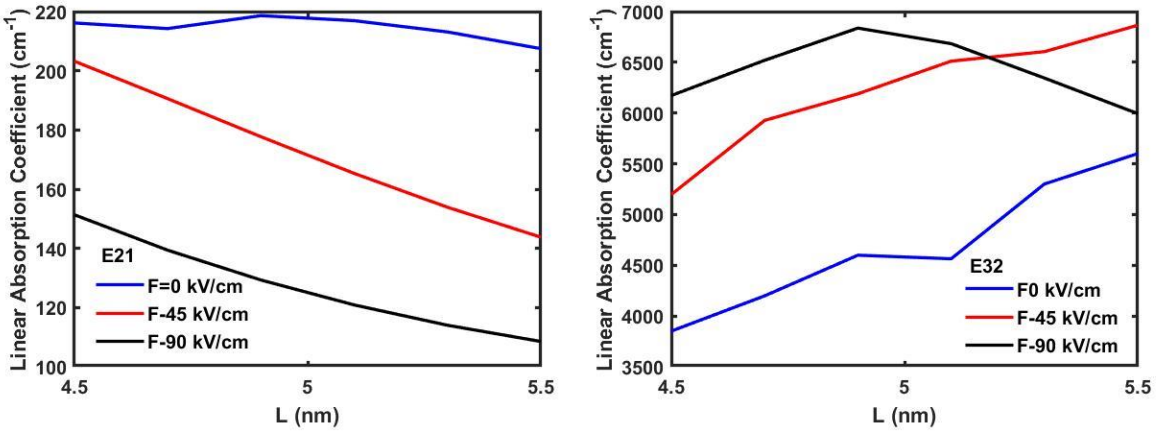

Figure 4. *L versus linear absorption coefficient for (a)* E_{21} *and (b)* E_{32} *for different electric field values.* $\sigma_v = 1\ x\ 10^{16}\ cm^{-2}$*is taken*

Same as electric field, maximum of the linear absorption coefficient for E_{21} transition is decreasing depending on the L under electric field (Figure 4) but it is almost constant for zero electric field. Increasing L increases linear absorption coefficient for zero and $-45\ \frac{kV}{cm}$ electric field intensities for E_{32} . But, it is first saturated and then decreasing for $-90\ \frac{kV}{cm}$ electric field intensity. Possible explanation of this behavior

is saturation in square of dipole matrix element for E_{32} as shown in Figure 2(b) under strong electric field intensity and small decrease in E_{32}.

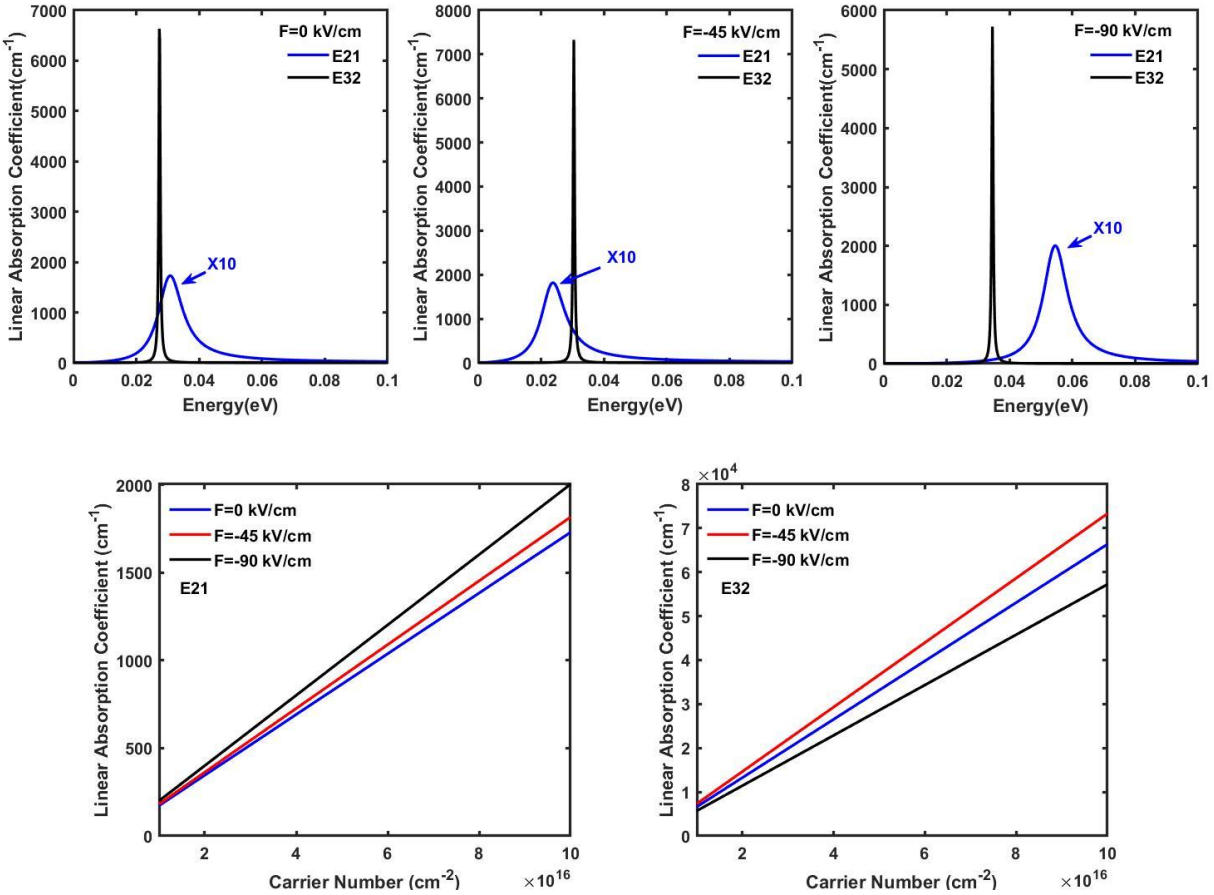

Figure 5. *Energy versus (a) linear absorption coefficient for injector region under different electric field intensity (upper) for $L = 5\ nm$ and $\sigma_v = 1\ x\ 10^{16}\ cm^{-2}$ and (b) carrier number versus linear absorption coefficient for $E_{21}$and E_{32}*

As shown in Figure 5(a), transition energy in injector region has blue shift with increased electric field due to rearrangement of electronic energy levels. Linear absorption coefficients for E_{21} are also relatively small compared with E_{32} even under electric field. In all cases, linear absorption coefficients are less than $100\ meV$ while radiative transition in gain region is $147\ meV$ (Figure 5(b)). Because of that injector region can cause strong internal absorption of radiative emission. That can cause a rapid decay in total output power. On the other hand, variation of carrier number enhances linear absorption coefficient for E_{21} and E_{32}. That can also turn down the benefit obtained by doping of injector region. So that doping has huge inverse impact on the optical properties. Excess of doping in the injector region can cause non-lasing while expecting enhancement.

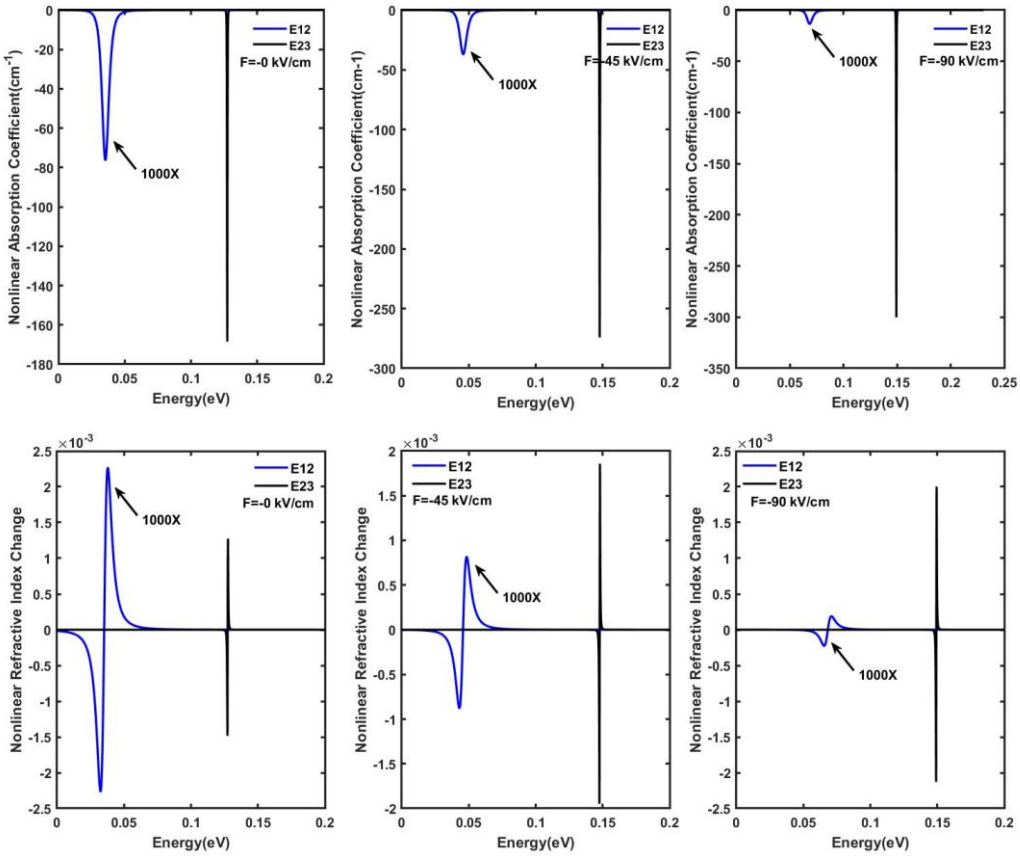

Figure 6. *Energy versus (a) nonlinear absorption coefficient (upper) and (b) nonlinear refractive index (lower) change for different electric field values in gain region.* $L = 5\ nm$ *and* $\sigma_v = 1\ x\ 10^{16}\ cm^{-2}$*are taken*

In this part of the paper, nonlinear optical properties of SL are investigated. Due to perturbative effect, calculations are done for optimized L and σ_v. Figure 6(a) shows nonlinear absorption coefficients depending on the applied electric field. It is seen that nonlinear absorption coefficient for E_{21} is decreasing due to lower square dipole matrix element with increased electric field. However, it is first increasing for E_{32} with applied electric field then it is almost constant for higher electric field intensity. That is important for stable laser performances. As seen in Figure 6(b), nonlinear refractive index change is negligible for E_{21} transition and nonlinear refractive index change for E_{32} is comparable with linear refractive index change in the gain region. Blue shift is also observed due to small deviation in transition energies under applied electric field for nonlinear absorption coefficients and nonlinear refractive index change. While blue shift is pronounced from 0 electric field to $-45\ kV/cm$, it does not change much after $-45\ kV/cm$ till $-90\ kV/cm$.

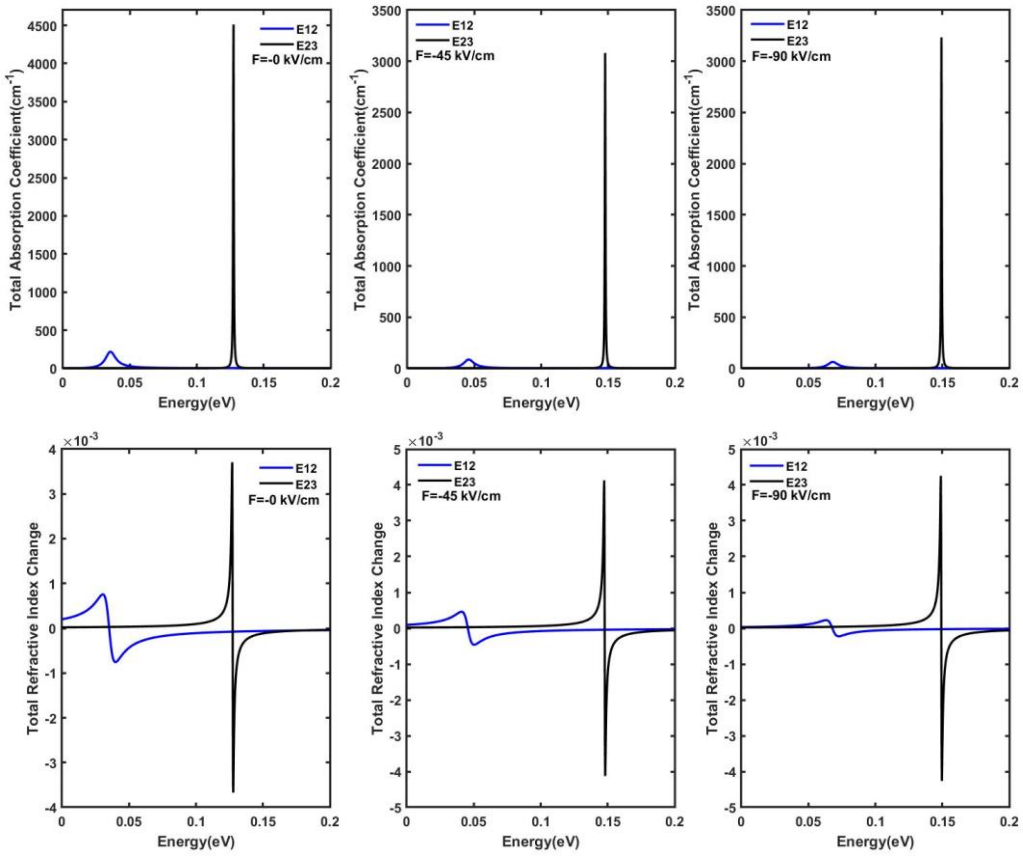

Figure 7. *Energy versus (a) total absorption coefficient (upper) and (b) total refractive index (lower) change for different electric field values in gain region.* $L = 5\ nm$ *and* $\sigma_v = 1\ x\ 10^{16}\ cm^{-2}$ *are taken*

Total absorption coefficients are calculated as shown in Figure 7(a), linear absorption coefficient is dominant as a result of lower contribution from nonlinear absorption coefficient as a perturbative term. It is seen that total refractive index change is negligible due to low carrier number in the gain region. That is very important conclusion in order to provide bias independent lasing.

In Figure 8(a), nonlinear absorption coefficients are given for injector region. Nonlinear absorption coefficient is very low for E_{21} transition. Nonlinear absorption coefficient for E_{32}transition is inversely proportional with electric field intensity. That is indication of lower internal absorption of laser light in the injector region during operation. Small amount of blue shift is also observed for E_{21} and E_{32} as in gain region. Same is in gain region refractive index change is also very low in the injector region. That is attributed with low doping of injector region because as given in Equation (9), nonlinear refractive index change is linearly proportional with carrier number.

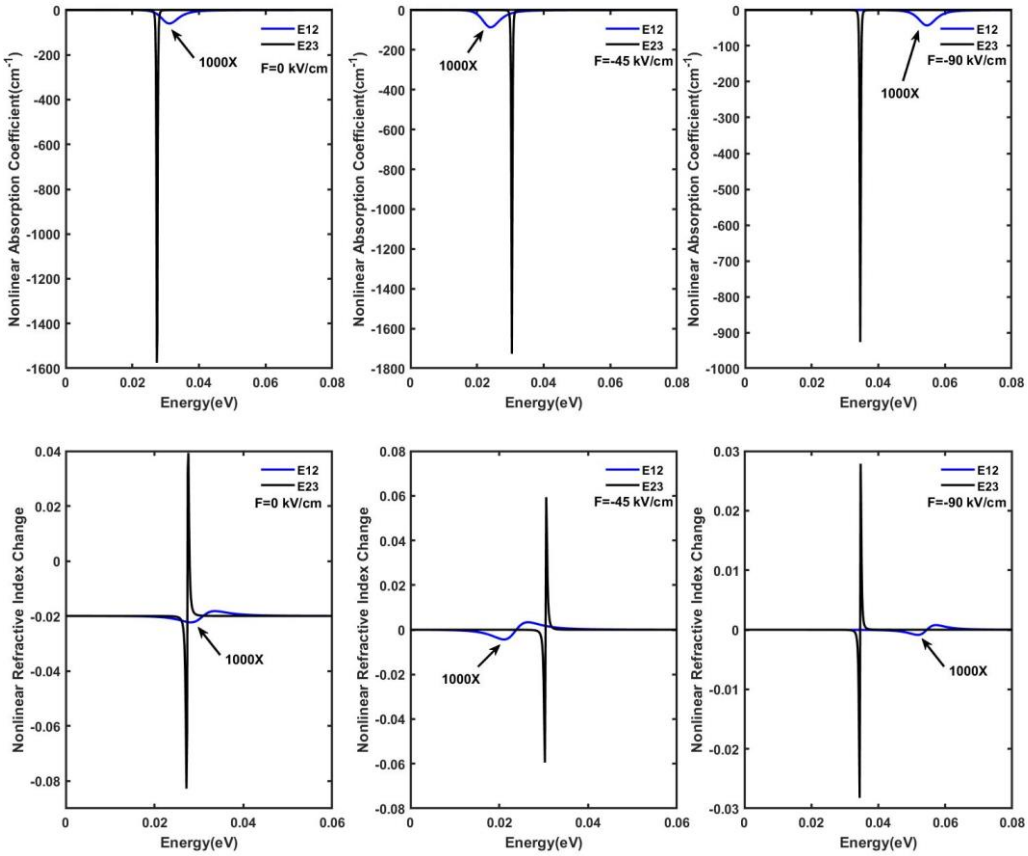

Figure 8. *Energy versus (a) nonlinear absorption coefficient (upper) and (b) nonlinear refractive index (lower) change for different electric field values in injector region.* $L = 5\ nm\ \ \sigma_v = 1\ x\ 10^{16}\ cm^{-2}$ *are taken*

In Figure 9, total absorption coefficient and total refractive index change are given. Even though blue shift is observed for E_{21} transition, total absorption coefficient is very low. Same shift is also observed for E_{32} and total absorption coefficient is first increasing than decreasing around 10% in the injector region. That can contribute higher laser performances at higher bias voltage. Total refractive index change is a few percent in the injector region under applied electric field and that will have small effect on device efficieny.

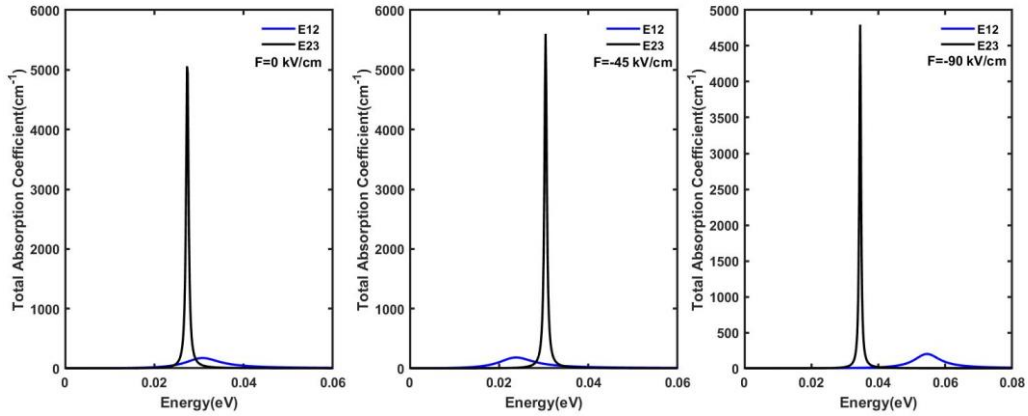

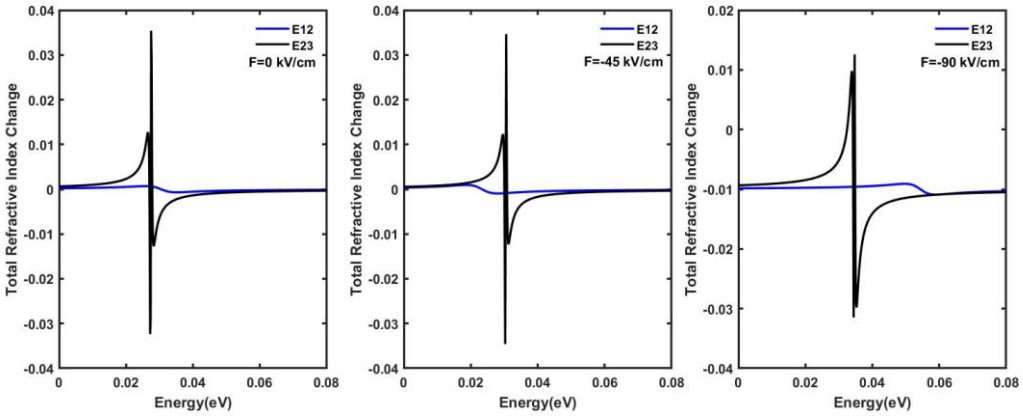

Figure 9. *Energy versus (a) total absorption coefficient (upper) and (b) total refractive index (lower) change for different electric field values in injector region.* $L = 5\ nm$ *and* $\sigma_v = 1\ x\ 10^{16}\ cm^{-2}$ *are taken*

4. CONCLUSION

In summary, optical and electrical properties of superlattice structure for quantum cascade laser applications are studied. Effect of last quantum well thickness (L) and carrier number under applied electric field are studied for active region of SL and effect of carrier number is studied for linear optical properties of the SL. After that nonlinear optical properties are investigated for constant superlattice thickness and carrier number. Total absorption coefficients and total refractive index change are found out. Finite difference method is used for obtaining wave functions and energy states under effective mass approximation. Even though electric field intensity and L have big impact on the distribution of energy states and square density matrix. Transition energies E_{21} and E_{32} are constant. $-45\ \frac{kV}{cm}$ electric field intensity and $\sim 5\ nm$ quantum well thickness are found as best parameters for highest radiative emission around $147\ meV$ for studied structure. Internal absorption of the radiative emission in injector region and gain region are possible. Doping of the injector region is very crucial and in case of heavy doping levels ($1\ x\ 10^{17}\ cm^{-2}$) to increase number of electron in circulation can destroy the benefit obtained from higher number of electron exist in radiative recombination. Effect of nonlinear absorption coefficient and nonlinear refractive index change are studied. It is seen that there is negligible effect of nonlinear refractive index change and nonlinear absorption coefficients are almost constant for different electric field intensities. As a conclusion, this study is exceptional due to considered effect and can contribute to literature while designing the laser gain and injector.

CONFLICTS OF INTEREST

No conflict of interest was declared by the author.

REFERENCES

[1] Yoffe, A. D., "Semiconductor quantum dots and related systems: Electronic, optical, luminescence and related properties of low dimensional systems", Advances in Physics, 50: 1, (2001).

[2] Vali, M., Dideban, D., Moezi, N., "A scheme for a topological insulator field effect transistor", Physica E, 69: 360, (2015).

[3] Kuo, D. M. T., Fang, A., Chang, Y. C., "Theoretical modeling of dark current and photo-response for quantum well and quantum dot infrared detectors", Infrared Physics & Technology, 42: 433, (2001).

[4] Zheng, J., Zhang, Y., Li L., Tang, S., Shi, Y., Chen, X., "An equivalent-stepped-index-coupled DFB semiconductor laser and laser array realized by stepping the duty cycle of the Sampled Bragg grating", Optics & Laser Technology, 67: 38., (2015).

[5] Karabulut, I., Mora-Ramos, M.E., Duque, C.A., "Nonlinear optical rectification and optical absorption in GaAs/$Ga_{1-x}Al_xAs$ asymmetric double quantum wells: Combined effects of applied electric and magnetic fields and hydrostatic pressure", Journal of Luminescence, 131: 1502, (2011).

[6] Martinez-Orozco, J.C., Mora-Ramos, M.E., Duque, C.A., "Nonlinear optical rectification and second and third harmonic generation in GaAs δ-FET systems under hydrostatic pressure", Journal of Luminescence, 132: 449, (2012).

[7] Dakhlaoui, H., Almansour, S., Algrafy, E., "Effect of Si δ-doped layer position on optical absorption in GaAs quantum well under hydrostatic pressure Superlattices and Microstructures, 77: 196, (2015).

[8] Tai, V. V., Khanh, N. Q., "Transport properties of the two-dimensional electron gas in wide AlP quantum wells including temperature and correlation effects", Physica E, 67: 84, (2015).

[9] Niculescu, E.C., Eseanu, N., Radu, A., "Heterointerface effects on the nonlinear optical rectification in a laser-dressed graded quantum well", Optics Communications, 294: 276., (2013).

[10] Gurnick, M.K., Detemple, T.A., "Two photon optical nonlinearities in a resonant quantum well system", IEEE Journal of Quantum Electronics,19: 791, (1983).

[11] Alaydin, B.O., Ozturk, E., Elagoz, S., "Interband transitions dependent on indium concentration in $Ga_{1-x}In_xAs$/GaAs asymmetric triple quantum wells", International Journal of Modern Physics B 32: 5, (2018).

[12] Nagahama, S., Iwasa, N., Senoh, M., Matsushita, T., Sugimoto, Y., Kiyoku, H., Kozaki, T., Sano, M., Matsumura, H., Umemoto, H., Chocho, K., Mukai, T., "High-Power and Long-Lifetime InGaN Multi-Quantum-Well Laser Diodes Grown on Low-Dislocation-Density GaN Substrates", Japanese Journal of Applied Physics, 39: L647-L650, (2000).

[13] Li, D., Sun, X., Song, H., Li, Z., Chen, Y., Jiang, H., Miao, G., "Realization of a High-Performance GaN UV Detector by Nanoplasmonic Enhancement", Advanced Materials, 24: 845–849, (2012).

[14] Bai, Y., Bandyopadhyay, N., Tsao, S., Selcuk, E., Slivken, S., Razeghi, M., "Highly temperature insensitive quantum cascade lasers", Applied Physics Letters, 97: 251104, (2010).

[15] Evans, A., Yu, J.S., Slivken, S., Razeghi, M., "Continuous-wave operation of λ∼4.8μm quantum-cascade lasers at room temperature", Applied Physics Letters, 85: 2166, (2004).

[16] Sirtori, C., Kruck, P., Barbieri, S., Collot, P., Nagle, J., Beck, M., Faist, J., Oesterle, U., "GaAs/$Al_xGa_{1-x}As$ quantum cascade lasers", Applied Physics Letters, 73:3486, (1998).

[17] Razeghi, M., Nguyen, B., "Band gap tunability of Type-II Antimonide-based superlattices", Physics Procedia, 3: 1207, (2003).

[18] Shi, J., Pan, S., "Calculation of linear and nonlinear intersubband optical absorptions in a superlattice with a step-well basis", Superlattices and Microstructures, 17: 1, (1995).

[19] Radu, A., "Laser-dressing of electronic quantum states in graded semiconductor nanostructures", Solid State Communications, 157: 11, (2013).

[20] Karimi, M.J., Vafaei, H., "Second-order nonlinear optical properties in a strained InGaN/AlGaN quantum well under the intense laser field", Superlattices and Microstructures, 78: 1, (2015).

[21] Zeiri, N., Sfina, N., Nasrallah S.A.B., Said M., "Intersubband resonant enhancement of the nonlinear optical properties in asymmetric (CdS/ZnSe)/X-BeTe based quantum wells", Optical Materials, 35: 875, (2013).

[22] Keshavarz, A., Karimi, M., "Linear and nonlinear intersubband optical absorption in symmetric double semi-parabolic quantum wells", Physics Letters A, 374: 2675, (2010).

[23] Rodriguez-Magdaleno, K., Martinez-Orozco, J., Rodriguez-Vargas, I., Mora-Ramos, M., Duque, C.A., "Asymmetric GaAs n-type double δ-doped quantum wells as a source of intersubband-related nonlinear optical response: Effects of an applied electric field", Journal of Luminescence, 147: 77, (2014).

[24] Safarpour, G., Izadi, M., Novzari, M., Yazdanpanahi, S., "Anisotropy effect on the linear and nonlinear optical properties of a lased dressed donor impurity in a GaAs/GaAlAs nanowire superlattice", Superlattices and Microstructures, 75: 936, (2014).

[25] Duque, C. M., Morales, A., Mora-Ramos, M., Duque, C. A., "Exciton-related nonlinear optical response and photoluminescence in dilute nitrogen cylindrically shaped quantum dots", Journal of Luminescence, 154: 559, (2014).

[26] Ungan, F., Pal, S., Mora-Ramos, M.E., Martinez-Orozco, J.C., "The electron-related optical responses for the square tangent quantum well: Role of applied external fields", Optik, 188: 12-18, (2019).

[27] Ungan, F., Pal S., Bahar, M.K., Mora-Ramos, M.E., "Nonlinear optical properties of morse quantum well modulated by THz laser fields", Physica E: Low-dimensional Systems and Nanostructures, 113: 86-91, (2019).

[28] Alaydin, B. O., "Effect of high bandgap AlAs quantum barrier on electronic and optical properties of $In_{0.70}Ga_{0.30}As/Al_{0.60}In_{0.40}As$ superlattice under applied electric field for laser and detector applications", International Journal of Modern Physics B, 2150027, (2020).

[29] Karabulut, I., Duque, C. A., "Nonlinear optical rectification and optical absorption in $GaAs–Ga_{1-x}Al_xAs$ double quantum wells under applied electric and magnetic fields", Physica E, 43: 1405, (2011).

[30] Chen, B., Guo, K., Wang, R., Zhang, Z., Liu, Z., "Linear and nonlinear intersubband optical absorption in double triangular quantum wells", Solid State Communications, 149: 310–314, (2009).

[31] Zhang, L., Yu, Z., Yao, W., Liu, Y., Ye, H., "Linear and nonlinear optical properties of strained GaN/AlN quantum dots: Effects of impurities, radii of QDs, and the incident optical intensity", Superlattices and Microstructures, 48: 434–441, (2010).

[32] Gambhir, M., Kumar, M., Jha, P.K., Mohan, M., "Linear and nonlinear optical absorption coefficients and refractive index changes associated with intersubband transitions in a quantum disk with flat cylindrical geometry", Journal of Luminescence, 143: 361–367, (2013).